**Title: Dynamic model of basic oxygen steelmaking process based on multi-zone reaction kinetics: Modelling of manganese removal**

**Author 1 (corresponding author)**

**Name:** Bapin Kumar Rout

**Affiliation**: Faculty of Science, Engineering and Technology, Swinburne University of Technology

**Mailing Address:** Hawthorn, Victoria, 3122, Australia, Email: brout@swin.edu.au

Phone: +61 3 9214 2837

**Author 2**

**Name:** Geoffrey Brooks

**Affiliation**: Faculty of Science, Engineering and Technology, Swinburne University of Technology

**Mailing Address:** Hawthorn, Victoria, 3122, Australia.

Phone: +61 3 9214 5672

**Author 3**

**Name:** M. Akbar Rhamdhani

**Affiliation**: Faculty of Science, Engineering and Technology, Swinburne University of Technology

**Mailing Address:** Hawthorn, Victoria, 3122, Australia.

Phone: +61 3 9214 8528

**Author 4**

**Name:** Zushu Li

**Affiliation:** WMG, University of Warwick

**Mailing Address:** WMG, University of Warwick, Coventry, CV4 7AL United Kingdom

**Author 5**

**Name:** Frank N.H. Schrama

**Affiliation:** Tata Steel, Netherlands

**Mailing Address:** Building 4H16, PO Box 10000, 1970 CA IJmuiden, NL

**Author 6**

**Name:** Willem van der Knoop

**Affiliation:** Tata Steel, Netherlands

**Mailing Address:** Building 4H16, PO Box 10000, 1970 CA IJmuiden, NL

## Abstract

In the earlier work, a dynamic model for the BOF process based on the multi-zone reaction kinetics has been developed. In the preceding part, the mechanism of manganese transfer in three reactive zones of the converter has been analyzed. This study identifies that temperature at the slag-metal reaction interface plays a major role in the Mn reaction kinetics and thus a mathematical treatment to evaluate temperature at each reaction interface has been successfully employed in the rate calculation. The Mn removal rate obtained from different zones of the converter predicts that the first stage of the blow is dominated by the oxidation of Mn at the jet impact zone, albeit some additional Mn refining has been observed as a result of the oxidation of metal droplets in emulsion phase. The mathematical model predicts that the reversion of Mn from slag to metal primarily takes place at the metal droplet in the emulsion due to an excessive increase in slag-metal interface temperature during the middle stage of blowing. In the final stage of the blow, the competition between simultaneous reactions in jet impact and emulsion zone controls the direction of mass flow of manganese. Further, the model prediction shows that the Mn refining in the emulsion is a strong function of droplet diameter and the residence time. Smaller sized droplets approach equilibrium quickly and thus contribute to a significant Mn conversion between slag and metal compared to the larger sized ones. The overall model prediction for Mn in the hot metal has been found to be in good agreement with two sets of different size top blowing converter data reported in the literature.

**Key words**: BOF, Mn refining, multi-zone kinetics, slag-metal emulsion, jet impact

## 1. Introduction

Manganese serves as an important alloying element in almost all commercial grades of steel. The presence of Mn can influence several critical properties of steel. High Mn can improve mechanical properties of steel, such as hardenability, toughness, and strength.[1] On the other hand, low Mn is required for ULC (ultra-low carbon) steels that require deep drawing applications. In many steel plants, manganese ore has been added to achieve high Mn at the end blow. This technique improves the process economics by reducing the addition of ferromanganese (FeMn) in the subsequent secondary steelmaking process. [1] On the other hand, some steel plants face the problem of high Mn (>1 wt pct) hot metal due to the use of lean iron ore having a high percentage of MnO in the blast furnace. [2] Processing of high Mn in BOF (basic oxygen furnace) is challenging as it causes problems such as slopping, refractory lining consumption, and yield losses. The manganese in such converters is refined by either overblowing oxygen or deslagging at the intermediate blow period. Therefore, it is very important to understand the manganese refining behaviour under blowing conditions in order to precisely control and improve the yield of Mn in a BOF process.

Several theoretical and experimental studies on the thermodynamics of manganese equilibrium between the metal and slag have been reported in the literature. [1, 3-7] As a result, numerous semi-empirical correlations describing the partitioning ratio of Mn ($L_{Mn}$) between the metal and slag containing manganese oxide are available in the literature.[1,3-11] Owing to the difficulty in measuring the Mn distribution ratio between the carbon saturated Fe and FeO bearing slag (due to CO gas bubbling), researchers often applied indirect experimental techniques to obtain the equilibrium data. Suito *et al.*[3-5], Jung [7], Kim *et al.*[8] and Morales *et al.*[1] developed equilibrium distribution models based on experimentally obtained data between liquid iron (Fe- Mn alloy) and slag. Another group of researchers used the equilibrium data between liquid Cu or Ag with slag to establish Mn distribution model for carbon saturated iron melts.[7,9] The above studies agree that the equilibrium Mn distribution between slag and metal increases with increase in total iron (T. Fe) in slag and decreases with increase in basicity (%CaO/%$SiO_2$). [3-11] Due to exothermic nature of Mn oxidation reaction, the negative effect of temperature on demanganisation has been reported.[3-6,11] It was further suggested that the Mn oxidation in a BOF operation is controlled by the oxygen potential determined by Fe/$Fe_tO$ equilibrium. [1,5] However, the above mentioned equilibrium distribution correlations are limited to specific slag systems and no universal model has been established.

Meanwhile, due to increasing demand for improving high manganese yield, the reduction mechanism of MnO by dissolved carbon in liquid iron has been investigated by several researchers. [12, 13, 14,15,16] According to proposed mechanism, MnO in the slag is reduced by Fe at slag/metal interface producing Mn and FeO. The iron oxide is further reduced by CO at slag/gas bubble interface to form $CO_2$ which subsequently reacts with the dissolved carbon at gas bubble/metal interface to regenerate CO.[13,14] Xu *et al.*[14] reported that the rate of MnO reduction in carbon saturated iron melt is limited by interfacial reaction (MnO +Fe = Mn +FeO) and proposed a second order kinetic equation to describe the reaction rate.

Shibata *et al.*[15] developed a kinetic model describing the simultaneous reaction between slag and multi component iron alloy by using two film theory and reported that the reduction of MnO is controlled by the transport process in slag phase. The study was focused on the evaluation of rate parameters such as slag-metal interfacial concentration and discussed the possible rate controlling steps for the reduction of MnO with the aid of the kinetic model. Similarly, Marissa *et al.*[16] applied the coupled reaction model to analyse the reduction rate of MnO in slag in terms of the slag basicity, initial Si and C in the liquid iron. The rate of MnO reduction was reported to increase with increasing the initial C concentration. The above mentioned studies are limited to laboratory studies and did not include the kinetics of Mn oxidation under oxygen blowing. Further, no validation of this kinetic model was attempted with the industrial scale furnaces.

A few researchers attempted to establish a kinetic model for Mn refining in industrial scale furnaces (BOF and EAF) by considering both the oxidation and reduction kinetics. [6, 17] Takaoka *et al.* [17] analysed the equilibrium driving force for the reactions and concluded that the competition between oxidation of Mn by gaseous oxygen and reduction of MnO by C decides the kinetics of Mn refining in combined blowing converter. The authors were able to establish a semi-empirical kinetic model that incorporates reduction and oxidation reaction. However, the role of slag FeO on manganese transfer was completely ignored in this study and the kinetic parameters were derived from fitting the plant data, which limits the model for applying in different converters.

The present kinetic model for Mn refining reaction is based on a multi-zone kinetic model proposed by the authors in the previous publication. [18] The details of the development of the dynamic model which includes the reaction kinetics of C, Si, Mn and P coupled with flux dissolution and FeO generation model has been already discussed in the paper. In the present model, the three reactive zones of the converter, e.g. jet impact zone, slag-bulk metal zone, and slag-metal emulsion zone have been considered for the refining of manganese. The simultaneous occurrence of oxidation and reduction reaction kinetics has been analysed in each zone. The rate of Mn refining in the emulsion zone has been simulated by using the previously developed mathematical model for residence time [19], droplet generation [20] and decarburisation model [21]. Using the rate model the relative contribution of different zones on refining of Mn was quantified. Using this Mn refining kinetic model, the dynamic evolution of Mn in the hot metal was estimated and the effect of process parameters on manganese refining kinetics has been evaluated. The overall rate model for Mn prediction has been validated by using two sets of industrial data obtained from a 200 t and a 55 t top blowing converters.

## 2. Manganese reaction kinetics in BOF

The behaviour of manganese refining profile commonly observed in basic oxygen furnace (BOF) shows rapid oxidation at the beginning followed by back reduction of Mn from slag to metal during the middle stage and finally some further oxidation at the end stage of the blow. [22-24] Several researchers reported that the transfer of Mn between hot metal and slag is controlled by the oxygen potential, determined by Fe/$Fe_tO$ equilibrium according to the following reaction: [1, 3, 9,13,14]

$$(FeO) + [Mn] = (MnO) + [Fe] \qquad (1)$$

Under the condition of mass transport control, it is assumed that the chemical reactions are fast and achieve equilibrium all the time at the slag-metal interface. Kawai *et al.*[25] and Shinozaki *et al.*[26] reported that the resistance to the mass transport of Mn in metal and slag phases are of similar order; suggesting that a mixed controlled mass transport can be suitable to describe the Mn refining kinetics at liquid iron and slag interface. **Figure 1** shows a schematic of the mechanism of mixed transport controlled Mn transfer across the metal–slag interface (e.g. metal droplet-slag or bulk metal- slag).

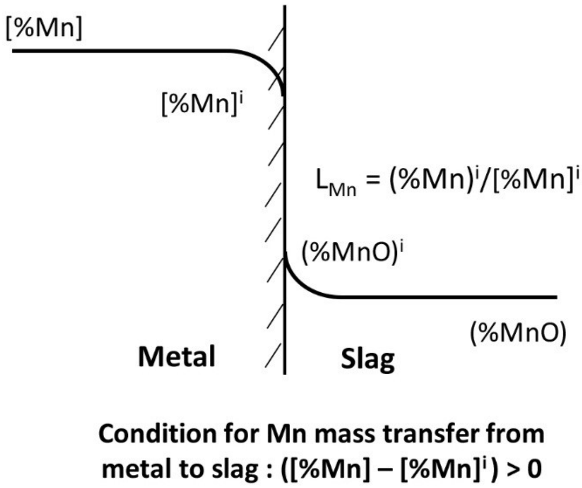


Figure 1: Schematic of mixed controlled Mn transfer across slag-metal interface

Accordingly, the rate equation for the mass transfer of manganese across the slag-metal interface can be written as:

$$-\frac{d[\%Mn]}{dt} = \frac{A}{W_m}\ k_m\rho_m\big([\%Mn] - [\%Mn]^i\big) \tag{2}$$

$$-\frac{d[\%Mn]}{dt} = \frac{A}{W_m}\ k_s\rho_s\big((\%Mn)^i - (\%Mn)\big) \tag{3}$$

and

$$-\frac{d[\%Mn]}{dt} = \frac{A}{W_m}\ k_o\rho_m\left([\%Mn] - \frac{(\%Mn)}{L_{Mn}}\right) \tag{4}$$

Where

$$k_o = \frac{k_m k_s \rho_s L_{Mn}}{k_m\rho_m + k_s\rho_s L_{Mn}} \tag{5}$$

Where $k_o$ is the overall mass transfer coefficient, k denotes the mass transfer coefficient, A is the area of the slag-metal interface, $\rho$ is the density, $L_{Mn}$ is the equilibrium distribution ratio, m and s denote metal and slag respectively.

As can be seen from Eq. 4, the thermodynamic driving force for the reaction, $\left([\%Mn] - \frac{(\%Mn)}{L_{Mn}}\right)$ is the only parameter that decides the direction manganese transfer i.e. whether Mn oxidises to slag or MnO reduces back to metal phase is primarily determined by the equilibrium distribution ratio, manganese oxide concentration in slag and Mn content in the hot metal.

Owing to the importance of evaluating manganese distribution between the metal and slag during steelmaking operations, several empirical correlations for the equilibrium partitioning ratio ($L_{Mn}$) and apparent equilibrium constant, $k'_{Mn}$ = %MnO /(%FeO×[%Mn]) as a function of slag composition and temperature have been developed by many researchers. Morales and Fruehan[1] indicated that $k'_{Mn}$ has greater practical use than $L_{Mn}$ since the expression incorporates the wt pct of FeO and thus can be used to evaluate the distribution of manganese at various oxygen potentials. For a known slag composition and temperature, $[\text{wt pct Mn}]^i$ can be evaluated from the empirical correlation of either $L_{Mn}$ or $k'_{Mn}$ and may be compared with the bath Mn concentration to estimate the reaction direction.

In order to examine the nature of Mn reaction, the authors compared the interfacial Mn concentration, $[wt\ pct\ Mn]^i$ calculated by the empirical correlations of $L_{Mn}$ with the actual [wt pct Mn] in the steel of a 200 t top blowing converter reported by Cicutti *et al.*[24] Suito's No. 2[4] and No. 3[3] model has been applied to estimate $L_{Mn}$. **Figure 2** shows the comparison of $[\%Mn]^i$ obtained from Suito's correlations with the bulk Mn concentration ($[\%Mn]^{act}$) during different stages of oxygen blowing. The analysis shows that, the interfacial Mn concentration is always lower than the measured Mn in the hot metal, indicating that the reaction at slag-metal interface has a positive thermodynamic driving force for forward direction and the flow of Mn takes place from bulk metal to slag throughout the blowing period. However, in the real process, the hot metal Mn profile shows the back reduction of manganese into the hot metal during the middle stage (4 min to 12 min) of the blow as observed by Cicutti *et al.*[24] Similar observation of Mn reaction and its deviation from equilibrium value has been reported by several authors. [17, 27] In the present work, the parameters responsible for this deviation have been subjected to investigation and discussed in the following sections.

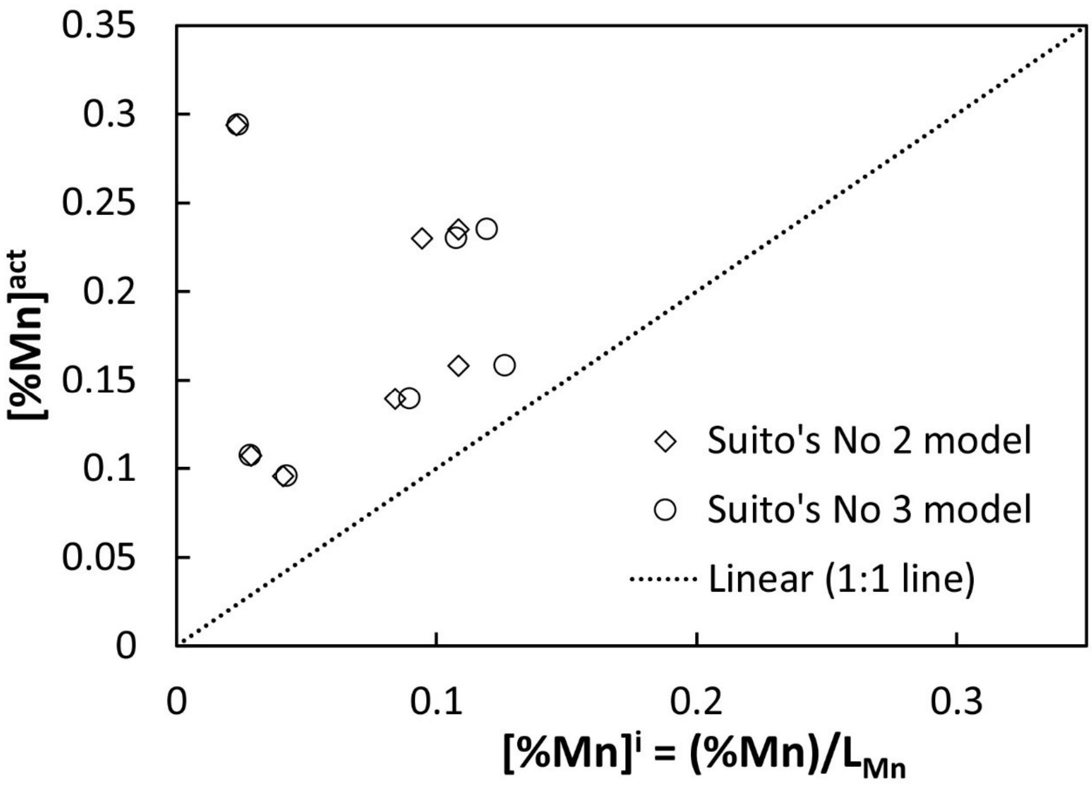


Figure 2: Comparison of actual Mn in the metal and the interfacial Mn calculated from Suito's equilibrium distribution models: Slag and hot metal composition data were taken from a top blowing process

## 2.1.Temperature at the reaction interface

The oxidation of manganese in the hot metal is an exothermic reaction and therefore $L_{Mn}$ is expected to decrease with increase in temperature. Zhu *et al.* [9] and Jung *et al.* [10] reported that the equilibrium distribution ratio of Mn decreases linearly with increase in metal bath temperature. The laboratory experiments studied for evaluation of $L_{Mn}$ are often performed in a crucible without oxygen blowing. Thus, the extraction and the extractive phases in the crucible experiments can be assumed to be in permanent contact with each other. Thermal gradient between the slag/metal interface and the bulk metal temperature can be thought to be negligible in those experiments. However, in a real BOF process, marked thermal gradient exists in the bath, the difference between the temperature of the top surface and bottom of the vessel can vary from 200 to 400 °C depending on the blowing type (soft or hard blowing). [28] A significant variation of temperature at the reaction interface (slag/metal) can make a potential change in the equilibrium concentration from the value obtained in laboratory scale $L_{Mn}$ correlations. Also, in a real BOF process, the reactions can take place in several reactive interfaces with different thermal conditions and phases. The slag/metal equilibrium alone may not accurately represent the overall thermodynamic driving conditions for the refining reactions in a BOF.

### 2.2. Competition between the reactions involving Mn

The mass transfer of manganese between metal and slag proceeds via several reactions i.e.

$$[Mn] + \frac{1}{2} O_2 = (MnO) \qquad (xx)$$

$$[Mn] + (FeO) = (MnO) + Fe \qquad (xx)$$

$$(MnO) + C = [Mn] + CO \qquad (xx)$$

It is entirely possible that the oxidation and reduction reaction of Mn takes place simultaneously in different zones and the balance between those rates decides the direction of overall manganese flow in the converter. A multiple zone reaction kinetics analysis may be appropriate to represent the overall process of Mn conversion between the metal and the slag.

### 2.3.Manganese reaction due to transitory phase contact in the slag-metal gas emulsion

The reactions occurring in the slag-metal emulsion are thought to take place at several interfaces with dynamic change in thermodynamic equilibrium and mass transfer conditions. [23, 29,30] As the droplets eject from the melt, a large number of distinct interfaces are created and the refining reaction in the emulsion proceeds via the reaction between the droplet and slag. It is observed that the kinetics of the refining reactions are a strong function of interfacial area, residence time, physicochemical condition of slag and droplet generation rate. Unlike the reactions occurring at a permanent phase boundary, only the equilibrium interfacial concentration cannot determine the direction of the mass conversion process between the hot metal and emulsion. The rate difference between the mass concentration of ejected and the refined droplets over the entire population of recirculated droplets would likely to determine the direction of mass transfer of Mn between hot metal and slag.

The discussion mentioned above, indicates that in a multi-zone reactor like BOF, caution must be taken in determining the transient rate parameters associated with Mn refining kinetics. In the present work, the mathematical treatments to the multi-zone reaction kinetics have been developed to simulate the time-variant rate parameters and overall Mn refining in the hot metal. Three reaction interfaces, i.e. (i) jet impact where the oxygen gas directly reacts with the hot metal bath, (ii) slag/ bulk metal interface where Mn in the hot metal reacts with the slag lying on the top, and (iii) in emulsion where the Mn reaction takes place due to transitory phase contact of the metal droplet with the slag, were considered for the formulation of the mathematical model. The effect of temperature on manganese equilibrium at each reaction interface was evaluated in the present work.

## 3. Kinetic modeling of manganese reaction

The primary regions for Mn reaction in BOF have been illustrated in **Fig. 3.** As can be seen from the figure, jet impact, slag- bulk metal and emulsion zones were considered to be the main zones for manganese refining.

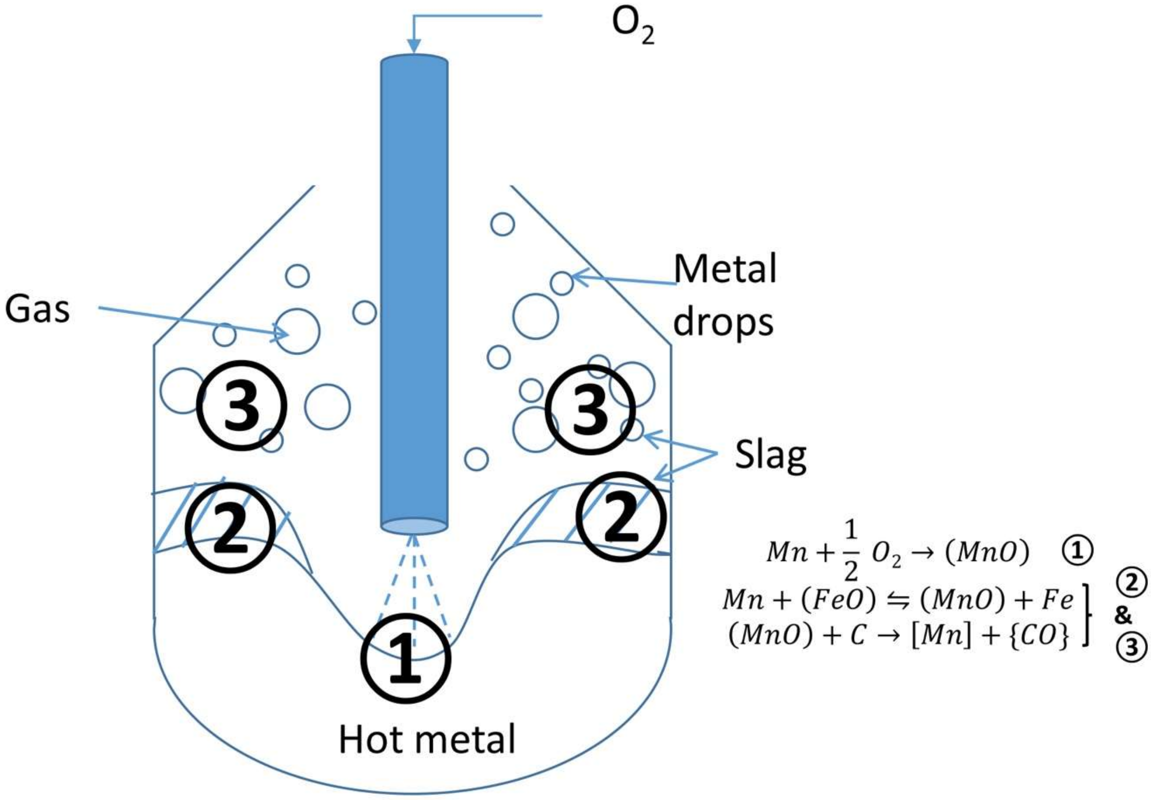


Figure 3: Schematic representation of oxidation/reduction reactions of Mn across various interfaces in a BOF

The reactive zones of manganese Mn refining are:

1. Jet impact zone

The direct oxidation of Mn by $O_2$ jet at the gas-metal interface can be given by the following reaction:

$$[Mn] + \frac{1}{2} O_2 (g) = (MnO) \quad (6)$$

2. Slag-bulk metal zone

In this reaction zone, a permanent phase contact between the slag and the metal can be assumed. Mn in the bulk metal reacts with FeO in the slag according to Eq. 1. This reaction can proceed either in the forward direction or backward direction depending on equilibrium value of Mn at the interface set by the temperature and slag compositions. A certain amount of MnO in the slag is expected to reduce by dissolved C in the melt at slag-metal interface according to the Eq. 7.

$$(MnO) + [C] = [Mn] + CO(g) \quad (7)$$

Since it is evident that the Mn equilibrium at the slag/metal is governed by Fe/$Fe_tO$ oxygen potential, the reduction of MnO by C has been ignored in the present work. [1, 5]

3. Slag-metal emulsion zone

In the emulsion zone, the ejected metal droplets are brought in contact with the slag and the reactions presented in Eq. 1 can be applied to evaluate the Mn reaction rate. The kinetic parameters of the total number, size evolution of metal droplets and time of residence in the emulsion are important parameters to be considered in order to determine the overall Mn refining by emulsion zone.

## 4. Mathematical modelling of overall Mn refining rate

The overall mass balance has been performed over the reacting zones to estimate the total Mn refining during the blowing process. The mathematical expression for the overall manganese refining rate can be written as:

$$\left(\frac{dW_{Mn}}{dt}\right)_{total} = \left(\frac{dW_{Mn}}{dt}\right)_{em} + \left(\frac{dW_{Mn}}{dt}\right)_{iz} + \left(\frac{dW_{Mn}}{dt}\right)_{sm} \qquad (8)$$

Here, $\left(\frac{dW_{Mn}}{dt}\right)_{em}$, $\left(\frac{dW_{Mn}}{dt}\right)_{iz}$ and $\left(\frac{dW_{Mn}}{dt}\right)_{sm}$ are the rate of Mn removed from the emulsion, jet impact and slag-bulk metal zones respectively (kg/s) . $\left(\frac{dW_{Mn}}{dt}\right)_{total}$ is the total rate of Mn refining at each time of blowing (kg/s).

The concentration of manganese in the bulk metal was calculated by the following mass balance equation:

$$W_b^{t+\Delta t} \times [wt\, pct\, Mn_b]^{t+\Delta t} = W_b^t \times [wt\, pct\, Mn_b]^t - \left(\frac{dW_{Mn}}{dt}\right)_{em} \times \Delta t - \left(\frac{dW_{Mn}}{dt}\right)_{iz} \times \Delta t - \left(\frac{dW_{Mn}}{dt}\right)_{sm} \times \Delta t + \left(\frac{dW_{Mn}}{dt}\right)_{sc} \times \Delta t \qquad (9)$$

Where $\Delta t$ is the numerical time step, $W_b^t$ is the weight of the hot metal (kg) at time t, $W_b^{t+\Delta t}$ is the weight of the hot metal at previous time step $(t + \Delta t)$, [wt pct $Mn_b$] is the weight percentage of Mn in the bulk metal, $dW_{Mn}/dt$ is the rate of Mn refining (kg/s) and the subscripts em, iz, sm and sc represents emulsion, jet impact, slag-metal bulk interface and scrap respectively.

The change in mass of the bulk metal has been estimated using the calculated mass of scrap, droplet generation and return to bath, slag and gas formation during time $\Delta t$. The mathematical expression can be written as:

$$W_b^{t+\Delta t} = W_b^t + \Delta W_{sc}^{m,t} - \Delta W_m^{sl,t} - \sum\left(\frac{dW_i}{dt}\right)_{em} \times \Delta t - \sum\left(\frac{dW_i}{dt}\right)_{iz} \times \Delta t \qquad (10)$$

Here $W_b^{t+\Delta t}$ is the weight of the bulk metal at time t + Δt, $W_b^t$ is the weight of the bulk metal at time step t, $\Delta W_m^{sl,t}$ is the weight of the elements in hot metal converts into slag (at slag-bulk metal interface) and $W_{sc}^{m,t}$ is the weight of the melted scrap during time step Δt. droplets $\left(\frac{dW_i}{dt}\right)_{em}$ and $\left(\frac{dW_i}{dt}\right)_{iz}$ are the rate of refining of hot metal impurities (kg/s) through emulsion and jet impact zone respectively.

### 4.1. Modeling of Mn reaction kinetics at jet impact area

The rate of Mn oxidation at jet impact area can be expressed as a first order rate law assuming the reaction to be controlled by mass transfer in the hot metal. It is due to the rapid dissolution of oxygen in the hot metal as a result of high temperature exhibiting at jet impact area. Also, the mass transfer coefficient in the gas phase is higher of a few orders of magnitude than in metal phase and a fast chemical reaction can always be expected at high temperatures. The liquid phase mass transfe controlled Mn refining rate equation in jet impact area can be written as:

$$\left(\frac{dW_{Mn}}{dt}\right)_{iz} = -\mathrm{k_m} \times \frac{A_{iz}}{100} \times \rho_m([wt\,pct\,Mn] - [wt\,pct\,Mn]_{iz}^{eq}) \qquad (11)$$

Here $\mathrm{k_m}$ is the mass transfer coefficient in hot metal, $A_{iz}$ is the area of the jet impact and $\rho_m$ is density of steel. The value of $[wt\,pct\,Mn]_{iz}^{eq}$ was estimated from the following chemical reactions:

$$[\mathrm{Mn}] + [\mathrm{O}] = (\mathrm{MnO}),\ \log K_{MnO} = 12760/T - 5.62 \qquad (12)$$

$$1/2\ O_2 = [\mathrm{O}],\ \log K_O = 6170/T + 0.125 \qquad (13)$$

The overall equilibrium constant for the Mn oxidation reaction according to Eq. 6 is given by:

$$\log K = \log K_{MnO} + \log K_{o} \tag{14}$$

Oxygen partial pressure, $P_{O2}$ is assumed to be 1 atm ($1.013 \times 10^{5}$ Pa) and activity of MnO, $a_{MnO}$ has been calculated by regular solution model introduced by Ban-Ya. [31] In a real BOF process the value of $P_{O2}$ will be much lower than the atmospheric pressure as the jet entrains a large amount of CO and $CO_2$. The assumption is initially undertaken to qualitatively analyse the behaviour of equilibrium driving force of Mn reaction at gas/metal interface. The measured thermal profile of hot spot reported by Chiba *et al.* [32] has been used to simulate the temperature in the jet impact area. It was assumed that temperature in the jet impact linearly increases from 2273K to 2573K during the first 25 pct of the blow. During the main blow period (25 pct to 80 pct of blow), it remains constant with a value of 2573K. Finally after 80 pct of oxygen blowing, the temperature was assumed to decrease linearly and equals the hot metal temperature at the end of refining. The calculated value of $[wt\ pct\ Mn]_{iz}^{eq}$ was found to be in the order of $10^{-4}$ to $10^{-5}$ for a 200 t converter (Cicutti *et al.* [24]). In a BOF process the Mn content in the hot metal usually varies from 0.3 to 0.6 wt pct, and the estimated equilibrium value was found to be 1,000 to 10,000 times lower than the actual manganese concentration. This ratio will further increase in an actual BOF process due to entrainment of $CO_2$ and CO gas ($P_{O2}<1$) and our assumption of $P_{O2}$ may not have large influence on the rate calculation. This low value of equilibrium concentration shows that the Mn oxidation reaction in jet impact area has a strong positive thermodynamic driving force for Mn refining from bulk metal.

Mass transfer in the metal phase has been assumed to be the rate controlling step for the Mn oxidation kinetics in the jet impact area. It is due to the rapid dissolution of O in the hot metal under extremely high temperature generated in the hot spot region. The mass transfer coefficient in the metal phase was assumed to be a function of the amount of stirring in the bath. Ishikawa [33] investigated the reaction kinetics in a top blowing test converter and reported that the kinetics of Si and Mn are a strong function of agitation in the bath and proposed a correlation for $k_m$ as a function of stirring energy, bath diameter and temperature. In the present work, the relationship proposed by Kitamura *et al.*[34], has been used to determine the mass transfer coefficient of Mn in the melt phase.

$$\log k_m = 1.98 + 0.5 \log\left(\frac{\varepsilon H^2}{100L}\right) - \frac{125000}{2.3RT} \tag{15}$$

where $k_m$ is the mass transfer coefficient in metal phase (cm/s), ε is the stirring energy (W/t), H and L are the bath depth (cm) and diameter of the furnace respectively and T is the temperature in the impact zone (K).The total stirring energy was calculated (see appendix A.1. for details) from the combined effect of the top and bottom gas injection in the BOF. [35]

One important parameter which controls the rate of Mn oxidation is the evolution of interfacial area available for gas-metal reaction at jet impact region. The gas-metal interfacial area was assumed to be the surface area of the cavity generated due to the impinging gas jet on the liquid metal. The calculation of jet cavity area as a function of blow parameters has already been discussed in the first part of the work. [18] For multi-head nozzles, the cavity coalescence was ignored and the overall cavity area was calculated by just adding the individual cavity formed by each nozzle.

### 4.2. Modelling of Mn reaction kinetics at slag-metal interface

The rate of Mn transfer across the slag-bulk metal interface as a result of the reaction between [Mn] in the bulk metal and (FeO) in the slag is assumed to be controlled by the transport of both [Mn] in metal and (MnO) in the slag. Several past studies reported that the resistance to mass transport of Mn in hot metal and slag are roughly at the same order of magnitude. [25,26]

In the present work, therefore, both resistance have been taken into account in the rate model of Mn at the slag-metal interface.

$$\left(\frac{dW_{Mn}}{dt}\right)_{sm} = -k_o^{sm} \times \frac{A_{sm}}{100} \times \rho_m \left\{[wt\ pct\ Mn] - \frac{(wt\ pct\ Mn)}{L_{Mn}}\right\} \tag{16}$$

Where $A_{sm}$ is the surface area at slag-bulk metal interface, $k_o^{sm}$ is the overall mass transfer coefficient. The overall mass transfer coefficient was evaluated by applying Eq. 5. $k_m$ was calculated from Eq. 15. The slag phase mass transfer coefficient was given by: [36]

$$k_s = a \exp\left(-\frac{37000}{RT}\right).\varepsilon^b \tag{17}$$

Where $k_s$ is the mass transfer coefficient in slag phase (cm/s), R: gas constant ($J.mol^{-1}K^{-1}$), $\varepsilon$ is the stirring energy (W/t), a and b are the empirical parameters, assumed to be 1.7 and 0.25 respectively.[36] Industrial measurement shows that the slag is about 20 to 100 K hotter than the hot metal. [37] For simplicity, a uniform slag temperature which is 100 K higher than the hot metal temperatuer has been assumed in the rate calculation at slag-bulk metal interface.

The manganese partitioning ratio at the interface between the slag and the metal can be defined as the ratio between the wt pct of Mn in slag to wt pct of Mn in the hot metal as:

$$L_{Mn} = \frac{(wt\ pct\ Mn)^i}{[wt\ pct\ Mn]^i} \tag{18}$$

The subscript i in Eq. 18 denotes the concentration at the slag-metal interface. Since the chemical reaction is fast at high temperature, the reaction species were assumed to attain equilibrium all the time at the interface. The interfacial concentrations described in Eq. 18 can be replaced by the equilibrium concentration for the calculation of $L_{Mn}$. Some studies have been performed in the past to investigate the thermodynamics of Mn equilibrium and several correlations for Mn partition ratio has been reported in the literature. [3-5] In the present work, Suito's model [3] has been chosen for the calculation of manganese equilibrium concentration. The empirical correlation of $k'_{Mn}$ proposed by Suito has been developed between liquid iron and $CaO$-$SiO_2$-$Fe_tO$ slag with MnO concentration varying up to 16 wt pct. Since in Cicutti's slag data the wt pct of MnO falls in the same range, the correlation can be suitable in evaluation of interfacial Mn concentration. The following empirical relationship was suggested by Suito *et al.* [3] to determine the apparent equilibrium constant and $[\%Mn]^{eq}$ at the interface between slag and bulk metal.

$$\begin{aligned}\log k'_{Mn} = -0.0180[(wt\,pct\,CaO) + 0.23(wt\,pct\,MgO) \\ + 0.28(wt\,pct\,Fe_tO) - 0.98(wt\,pct\,SiO_2) \\ - 0.08(wt\,pct\,P_2O_5)] + \frac{7300}{T} - 2.697\end{aligned} \quad (19)$$

Where the apparent equilibrium constant $k'_{Mn}$ is defined as:

$$k'_{Mn} = \frac{(wt\,pct\,MnO)}{(wt\,pct\,T.Fe) \times [wt\,pct\,Mn]} \quad (20)$$

The interfacial area between slag and bulk metal ($A_{sm}$) was calculated by subtracting the cavity area resulted by top jet from the geometrical area of the bath surface. For non-coalescence cavity the area of slag metal can be expressed by the following equation:

$$A_{sm} = \pi\,(\frac{D_b^2}{4} - n_n \times r_{cav}^2) \quad (21)$$

Here $D_b$ is the diameter of the bath surface (m), $n_n$ is the number of nozzles in the lance tip and $r_{cav}$ (m) is the radius of a single jet cavity. The cavity geometry was calculated by using the dimensionless relationships suggested by Koria and Lange.[38] In the above calculation, for simplicity, the surface area of the slag-bulk metal interface was assumed to be flat and the bath oscillation was neglected.

### 4.3. Modelling of Mn reaction kinetics in slag-metal emulsion

#### 4.3.1. Microkinetics: Evaluation of Mn refining rate in a droplet

Similar to slag-bulk metal zone, the reaction of Mn at metal droplet and slag interface was considered to be controlled by the transport of Mn inside the metal drop and MnO in the slag. [39] Thus, a mixed controlled kinetic equation has been applied for evaluating the rate of reaction of metal droplets in the slag-metal emulsion. **Figure 4** illustrates the schematic of exchange of Mn between metal-drop and slag inside the emulsion phase. The rate of Mn removal by a single droplet can be expressed as:

$$\left.\frac{d[wt\ pct\ Mn]}{dt}\right|_{drop}^{em} = -\frac{A_{drop}}{V_{drop}} \times k_o^{em} \times \left\{[wt\ pct\ Mn] - \frac{(wt\ pct\ Mn)}{L_{Mn}}\right\} \qquad (22)$$

$A_{drop}$ and $V_{drop}$ are the area and volume associated with the single droplet in the emulsion and $L_{Mn}$ is the equilibrium partition ratio of Mn between slag and metal droplet. Similar to the slag-bulk metal interface, $L_{Mn}$ was calculated by applying Eq. 18 at slag- metal droplet phase boundary. Instantaneous surface area of the droplet due to bloating behaviour resulted by decarburization reaction has been estimated from the empirical correlation of density change of droplet as a function of decarburization rate and FeO wt pct in slag proposed by Brooks *et al.* [19]

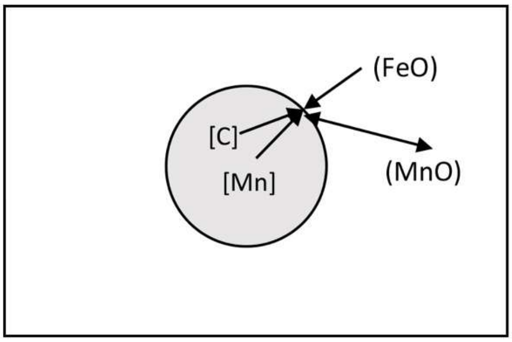


Figure 4: Transport process of Mn at metal droplet and slag containing iron oxide interface in the emulsion zone

The overall mass transfer coefficient, $k_o^{em}$ was calculated by applying mixed controlled kinetics as mentioned in Eq. 5. It should be noted that the reaction at slag-metal droplet interface undergoes a transitory phase contact during the emulsion where as a permanent phase contact can be assumed between metal and bulk slag. The mass transfer coefficient of Mn transport in the metal for a translating droplet was determined by employing surface renewal model as

$$k_m^{drop} = 2 \times \sqrt{\frac{D_{Mn}}{\pi\, t_c}} = 2 \times \sqrt{\frac{D_{Mn} u}{\pi\, d_p}} \qquad (23)$$

Here $d_p$ is the average droplet diameter (m) corresponding to the same size class and u is the velocity (m/s) of the metal droplet in the emulsion. $D_{Mn}$ is the diffusion coefficient of Mn in molten metal ($m^2/s$). The temperature and viscosity effect on mass diffusivity was taken into account by applying the Stokes-Einstein equation.

$$D_T^{Mn} = D_{1873}^{Mn}\left(\frac{T}{1873}\right) \times \left(\frac{\mu_{m,1873}}{\mu_{m,T}}\right) \qquad (24)$$

Where $D_T^{Mn}$ is the diffusivity of Mn in hot the metal of temperature T ($m^2/s$), ${D^{Mn}}_{1873}$ is the diffusivity of species at T =1873K ($m^2/s$), T is the temperature (K), $\mu_{m,1873}$ and $\mu_{m,T}$ are the viscosity of hot metal at 1873K and T respectively. In the present work, the effect of temperature on viscosity has been neglected.

On the slag side, the mass transfer coefficient can be calculated assuming the metal droplet to be a rigid sphere with a stream of slag surrounding it. Due to high Schmidt number prevailing in steelmaking slag (in the range of $10^5$ and $10^6$ in slag as compared to ~$10^3$ in steel melt) , the boundary layer is considered to be laminar and the effect of turbulence on mass transfer coefficient can be neglected.[39] The mass transfer coefficient in slag phase was determined by the following relationship[39]:

$$Sh = 2 + 0.6Re^{1/2}Sc^{1/3} \tag{25}$$

Where Sh is the Sherwood number, Re is the Reynolds number and Sc is the Schmidt number. The diffusion of MnO in slag $D_{slag}$ was taken to be $5x10^{-10}$ $m^2/s$. [39]

As different sizes of metal droplets are ejected from the melt, the size distribution and time of residence are important parameters to estimate the kinetics of refining of Mn. The authors in their previous publications [18,20] have developed mathematical models to predict the amount of ejected droplets, size distribution and residence time as a function of the furnace operating parameters, hot metal and slag compositions. The size distribution of the entire population of ejected droplets was divided into different groups by using Rosin-Rammler-Sperling (RRS) distribution function. [40] The mathematical model for the residence time of the metal droplets was based on the principle of ballistic motion, proposed by Brooks *et al*.[19] The trajectory of a droplet in both vertical and horizontal direction was calculated by the force balance method with taking into account the dynamic change in density due to bloating caused by the nucleation of CO gas bubbles. The details of the development of residence time submodels can be found elsewhere. [18] The residence time model calculates the concentration change of Mn (also C, Si and P) in the droplet for a particular size class at each time of its trajectory inside emulsion. At each numerical time steps, the Mn concentration of each size group of the droplets at the time of their re-entry to the bath was evaluated.

### 4.3.2. Temperature at metal drop-slag interface

As described in the previous work [18] the temperature at metal droplet-slag interface was estimated by assuming the ejected droplets to be rigid spheres and initially carry the temperature of the hot spot. The droplets gradually decrease the temperature as they pass through the emulsion phase which is expected to be a lower temperature than the hot spot. A homogeneous temperature in the emulsion, same as of the slag has been assumed in the calculation. The following equation has been applied to determine the droplet interface temperature:[41]

$$T_{drop} = T_0 + \frac{T_0 - T_\infty}{1 + \beta} \tag{26}$$

$$\beta = \left( \frac{\lambda_m C_{p,m} \rho_m}{\lambda_s C_{p,s} \rho_s} \right)^{1/2} \tag{27}$$

where $\lambda$ is the conductivity (W/mK), $C_p$ is the heat capacity (J/kg). The subscript m, s corresponds to hot metal and slag. $T_{drop}$, $T_0$, $T_\infty$ represents the temperature at the droplet interface in the emulsion, temperature of the droplet at the time of ejection and the emulsion temperature respectively. Here $T_0 = T_{iz}$ and $T_\infty = Ts$, are assumed for the calculation of the temperature at the droplet interface. The details about the calculation of heat capacity in metal ($C_{p,m}$) and slag ($C_{p,s}$) phases can be found in an earlier publication.[18]

### 4.3.3. Macrokinetics: Evaluation of overall Mn refining rate by emulsion phase

The overall Mn removal rate by emulsion at each time of blowing was calculated by the difference between the total mass of droplet ejected and returning droplets at a predefined numerical time step.

$$\left(\frac{dW_{Mn}}{dt}\right)_{em} = \frac{W_{Mn}^{eject,t} - W_{Mn}^{return,t}}{\Delta t} \tag{28}$$

The total mass of manganese (kg) ejected into the emulsion was estimated from the previously developed droplet generation model. [20]

$$W_{Mn}^{eject,t} = \left(\sum_{p=1}^{P} \left(R_{B,T}\right)^{t}{}_{p} \times \Delta t\right) \times \frac{[wt\ pct\ Mn]^{t}{}_{m}}{100} \tag{29}$$

Where P is the total number of divisions of the ejected droplet size spectrum, $\left(R_{B,T}\right)^{t}{}_{p}$ is the rate of droplet generated (kg/s) for a given size class $p$ at time t and $[wt\ pct\ Mn]^{t}{}_{m}$ is the concentration (wt pct) of Mn in the hot metal. The value of total division in the size spectrum, P was taken to be 6 in the present model calculations.

Micro-kinetic model estimates the manganese concentration of an individual droplet at each time of its trajectory inside the emulsion phase. For each size group, the final Mn concentration at the time of their return to the bath and the total time of residence in the emulsion was calculated. The total number of returning droplets having the final manganese concentration at the time of their re-entry to the hot metal has been estimated and the total weight of Mn entering into the bath was calculated.

$$W_{Mn}^{return,t} = \sum_{p=1}^{P} N^{return,t}{}_{p} \times \frac{[wt\ pct\ Mn]_{d,p}^{t_{res}} \times w_{d,p}^{t_{res}}}{100} \tag{30}$$

Here, $N_p^{return,t}$ is the number of returning metal droplets, $[\text{ wt pct } Mn]_{d,p}^{t_{res}}$ and $w_{d,p}^{t_{res}}$ are the concentration of Mn and the weight (kg) of a droplet for a given size class at the time of its re-entry to the molten bath at a given blowing time, t.

## 5. Model assumptions and input data

The following are the list of assumptions, which has been made in developing the kinetic model for demanganisation in a BOF process.

1. The mass transfer of manganese only takes place at three reactive zones i.e. (i) jet impact area, (ii) slag-bulk metal, and (iii) slag-metal-gas emulsion.
2. The manganese refining in the slag-metal emulsion and slag-metal bulk zone was assumed to be proceeded by Mn and FeO reaction.
3. The equilibrium manganese distribution ratio ($L_{Mn}$) between the metal droplet and slag was assumed to be the same as between bulk metal and slag. Suito's empirical correlation of $L_{Mn}$ was considered for the calculation of manganese equilibrium at metal droplet -slag interface in the emulsion phase.
4. A linear hot metal temperature profile which varies between 1623-1923 K (1350-1650 °C) for Cicutti's heat data[24] and between 1603-1973 K (1330-1700 °C) for Holappa's data [42] has been used in the model calculations. The authors acknowledge that a linear temperature profile is a simplified assumption and type of additions (flux, iron ore) can have a significant effect on the thermal profile of the melt and need to be taken into account in the future dynamic model.
5. As reported by Cicutti *et al.*,[24] the initial droplet size spectrum was assumed to vary between $2.3\times 10^{-4}$ m to $3.35\times 10^{-3}$ m. The entire size range of droplets has been divided into different sizes groups and an average weight of droplets corresponds to each group was estimated by applying Rosin- Rammler- Sperling (RRS) distribution function. [39]

The details about the size distribution model of ejected droplets can be found in a previous study by Rout *et al.* [18] Six size groups of different droplet size ranges have been considered for the present model calculations.

The experimentally measured data from a 200 t combined blowing converter [24], and a 55 t top blowing converter [42] was used for model validation. In both the furnaces, samples of metal and slag are collected during seven different times of blowing from the start of the blow. For the 55 t converter data reported by Holappa *et al.*, [42] the precise information about the time and amount of flux addition during the converter operation was not found. Apart from the addition of lime and converter dust, fluorspar, bauxite and calcium borate was reported to use as a fluxing agent in the converter operation. Due to unavailability of the precise information about the time of addition of these flux materials, a predictive slag model could not be possible for Holappa's data.

Thus in the kinetics analysis of manganese refining for Holappa's data, the measured slag data at different time intervals of blowing period have been used through an interpolation technique as input in each step of model calculations. However, for the model used for Cicutti's data, a dynamic slag generation model that includes the evolution of iron oxide in slag based on oxygen mass balance and flux dissolution model have been incorporated. The model details can be found in our earlier publication. [18].

**6. Computational strategy**

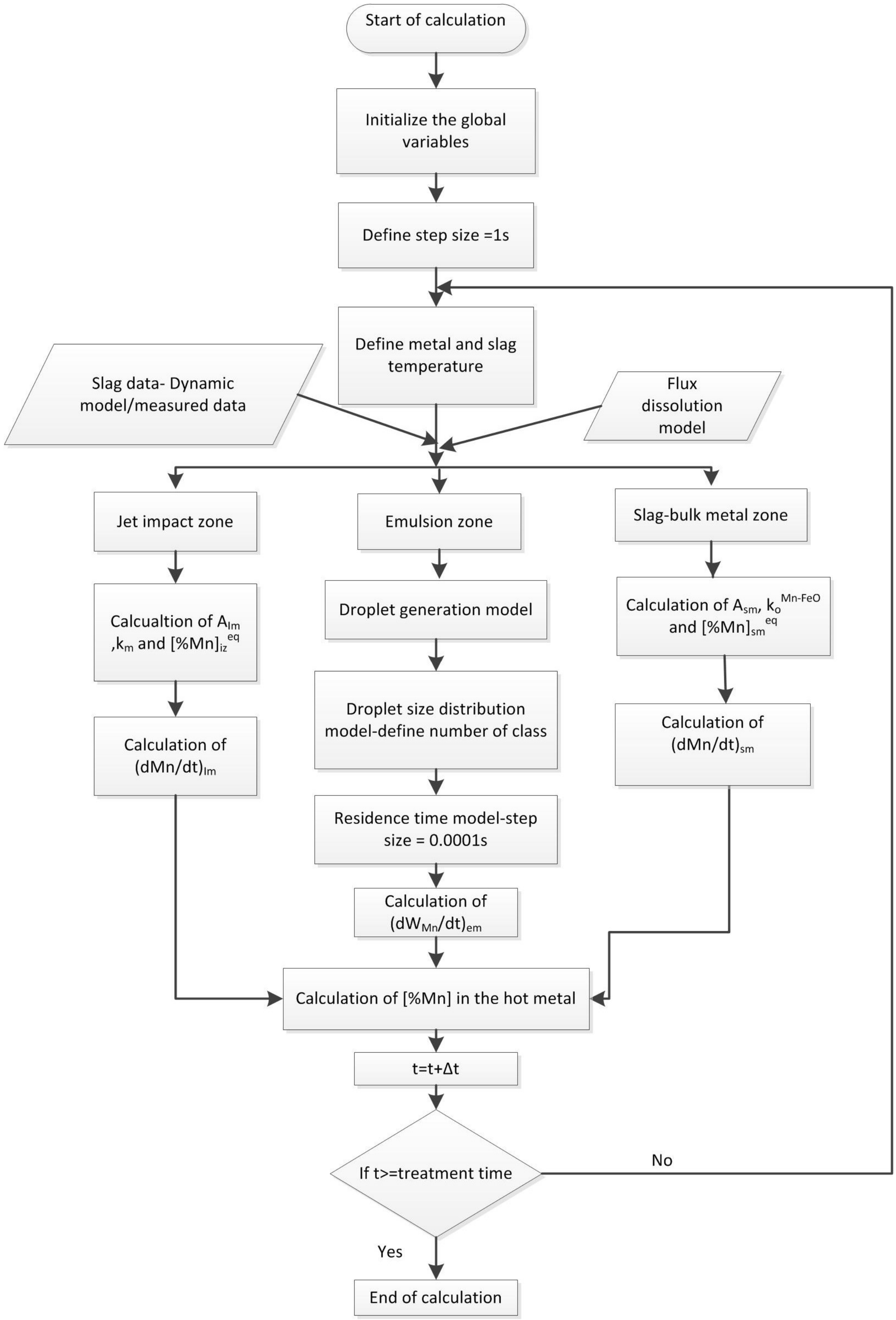


Figure 5: Calculation steps for Mn refinement model for a BOF process

The computational program uses finite difference method to compute the concentration of manganese in the hot metal in the next time step by using the known data in the previous time step. The simulation starts at blowing time of 2.2 minutes because only data is available at this time. All the initial inputs are entered into the model at this time. An optimum time step of 1s is chosen for calculation of bath Mn concentration. For the 55 t converter, the slag composition at each time step of calculation was calculated by using interpolation between the measured data points. These slag composition data were dynamically entered into the model as an input at each time step. However, in the 200 t converter, a dynamic slag generation model [18] was coupled with the model for the estimation of bulk Mn concentration at each computational time step.

Figure 5 demonstrates the algorithm of the mathematical model used for computing the change in manganese concentration in the bulk metal. Initially, the global input variables such as gas constant, molecular weight, lance profile, top and bottom flow rate, hot metal weight were entered into the central model. The scrap dissolution model, based on the previous model results by Dogan *et al.*[43], was assumed that 30 t of scrap in Cicutti's heat dissolute at a constant rate within the first seven minutes of the blow. The temperature profiles in the hot metal, slag and in the jet impact area were estimated based on predefined functions. The temperature at the slag-droplet interface was calculated by applying Eqs. 26 and 27. The physical properties such as density and viscosity of slag were estimated as a function of their composition and temperature. The density of slag at each time step was calculated using partial volume method[44] and modified Urbain model[45] was applied to estimate the slag viscosity.

Flux dissolution (lime and dolomite) rate was calculated as a function of temperature and physical properties of slag and metal. Previously developed flux dissolution model by Dogan *et al.*[46] was applied in the present work to determine the amount of dissolved flux in slag at each numerical time step. In the calculation of manganese refining rate in emulsion zone, the overall size spectrum of droplets has been divided into six classes, and the degree of manganese refining was calculated individually for each class by use of microkinetics sub-model discussed in section 4.3.1. An optimum numerical time step of 0.0001s, as already discussed in our previous work[18], has been chosen to calculate the residence time of the metal droplets in each class of diameter. By use of the droplet-generation sub-model[20], the total weight of the Mn in the droplet ejects into the emulsion phase was estimated by using Eq. 29. The total amount of manganese returning to the bulk metal after refining by the emulsion was determined by summing the weight of Mn in the entire population of returning droplets (Eq. 30). The total Mn refining rate through emulsion zone was estimated from the difference between the ejected mass of Mn and their return to the emulsion, as shown in Eq. 28. Similarly, sub-models to calculate the rate of Mn removal from slag-bulk metal and jet impact zone were developed by applying Eq. 11 and Eq. 16. Through Eq. 8-10, the rate of Mn refined from all the zones were combined, and mass balance has been performed to estimate the change in concentration of manganese in the hot metal. All the numerical computation has been carried out by using MATLAB® version 2016a. The model input parameters used in the calculation for the two different converters are listed in Appendix A.2. (Table A1 and Table A2).

## 7. Results and Discussions

### 7.1. Analysis of oxidation and reduction reaction of Mn in a BOF

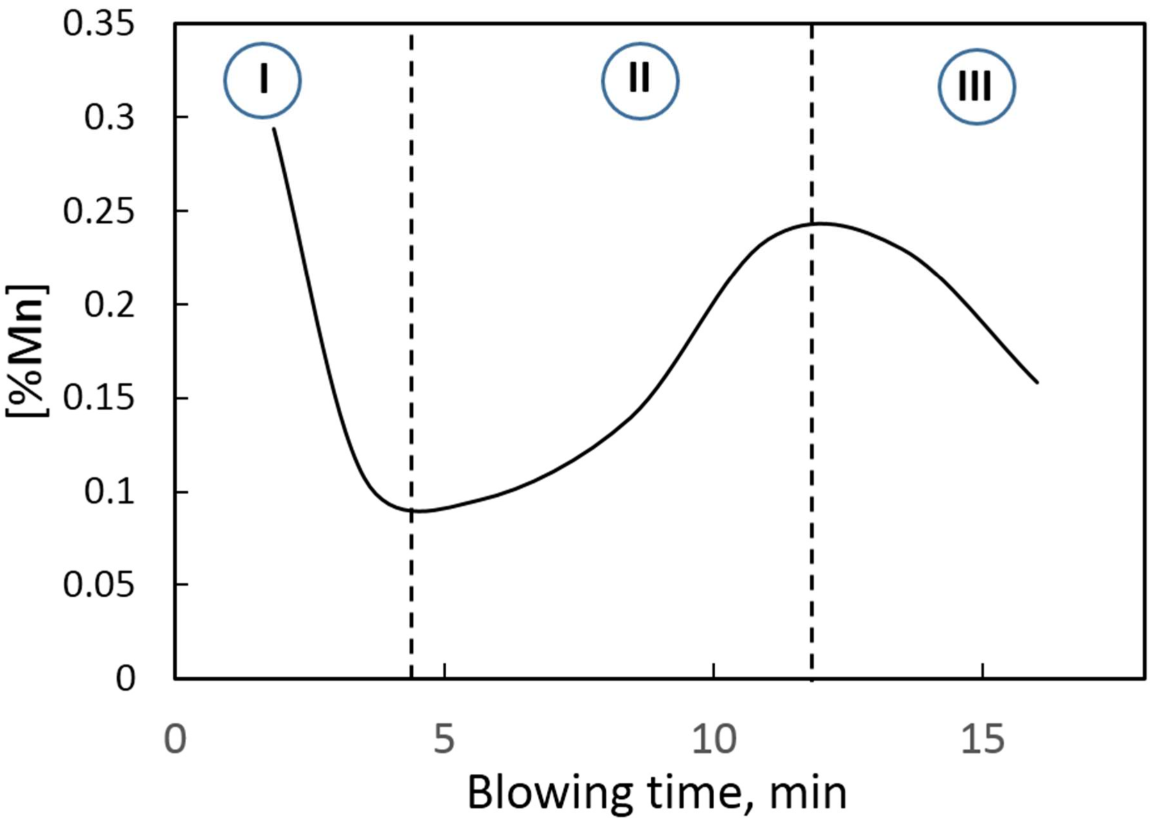


Figure 6: Typical manganese refining path in a top blowing converter.[22,24] Region I: rapid manganese oxidation, Region II- manganese reversion from slag to metal, Region III: manganese oxidation

A typical variation of Mn concentration in the hot metal during the blow period is shown in **Fig. 6.** [22, 24] The evolution of Mn in the molten bath can be broadly divided into three stages: (1) rapid oxidation of Mn from the hot metal at early stage of blow, (2) reversion of Mn from slag to metal during the middle stage of blowing, and (3) finally Mn oxidation towards the end blow period. As discussed in the earlier sections, manganese reaction primary takes place either by direct reaction with $O_2$ or with FeO in the slag. The competition between these reactions determines the overall rate and direction of Mn mass transfer.

The equilibrium Mn concentration at different interfaces has been calculated as a function of slag composition and temperature. The estimated value of [wt pct Mn]$^i$ at the gas-metal interface in jet impact zone was found in the order of $10^{-5}$, which implies that the reaction at the jet impact region has a strong positive driving force for Mn oxidation.

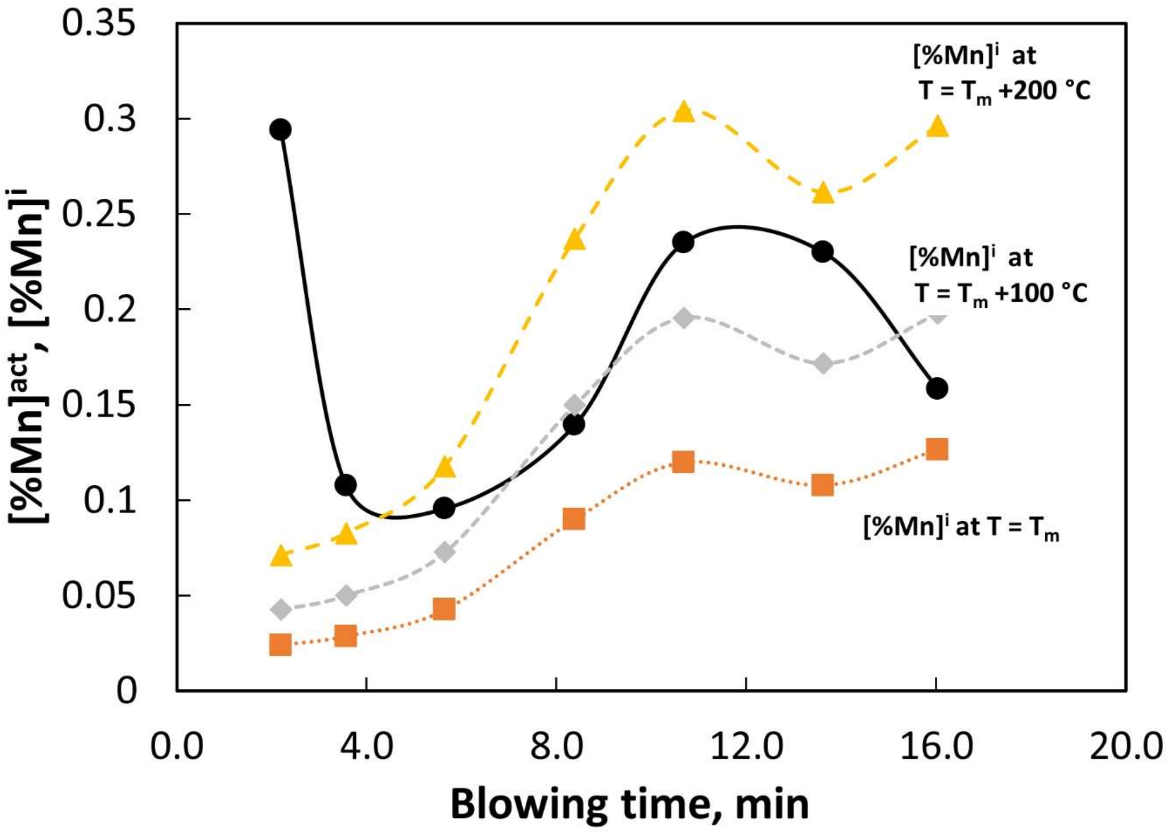


Figure 7: Effect of temperature on the equilibrium manganese at slag-metal interface (solid line- actual Mn in bath, dotted line- interfacial Mn concentration estimated at different slag-metal interface temperatures, $T_m$- Hot metal temperature (as measured during blowing time) and T is the interface temperature

However, the value of the interfacial concentration of Mn calculated by considering Mn/MnO equilibrium at slag/metal interface was found to have values in the same order as the manganese concentration in the hot metal bath. Since the metal droplets are originated from the periphery of jet impact region, it is likely that the interface between the metal droplets and slag may experience higher temperature than the bulk metal. Similarly, as reported in previous studies, the bulk-metal and slag interface can exhibit higher temperature than the bulk melt; a difference of 200 to 400 °C between the surface and bottom of the vessel has been reported by Rote and Flinn.[28] The effect of temperature on the equilibrium concentration of Mn at slag/metal interface has been illustrated in **Fig. 7.** It should be noted that the slag concentration is changing during the blow period according to the measured values in the Mn equilibrium calculation.

When the temperature of the interface was maintained as the bulk metal temperature the equilibrium line was found to be always lower than the actual Mn in the metal. In spite of the change in oxygen potential (slag composition) and hot metal temperature in the calculation, the shape of the bulk Mn concentration was not explained by the predicted equilibrium concentration. However, as the interface was raised to 100 °C above the bulk temperature the value of $[\text{wt pct Mn}]^i$ was increased above the bulk Mn concentration and some reversion was found during the intermediate stage of blowing. Further, the oxidation of Mn during the early blow and reversion after 5 min of the blow was noticed when the temperature of the droplet/slag interface was raised to 200 °C above the bulk metal temperature. The change in the direction of equilibrium driving force was undoubtedly noticed when the temperature of the interface increased. In the earlier publication, the authors have mapped the variation of the temperature profile in different interfaces of the converter during the blowing period. [18] It was observed that the droplet surface exhibits 90 to 200 K higher temperature than the hot metal. The droplet surface temperature was predicted to increase linearly in most part of the blow, expect towards the end blow a decreasing trend is observed due to a reduction in hot spot temperature. Therefore, it may be inferred that the high temperature prevailing at the reaction interface at the droplet-slag interface is one of the significant factors that control the oxidation and reduction behaviour of manganese in the top blowing process.

Based on our understanding of manganese equilibrium for the reactions described in Eq. 1 and Eq. 6, the kinetics of manganese transfer can be qualitatively evaluated. Table 1 summarizes the reactions involving Mn and their direction during the different stages of the BOF operation.

### 7.2. Mn refining in different reactive zones in the converter

The rate of manganese refined by the three distinct zones inside the BOF converter as a function of blowing time has been shown in **Fig. 8**. In the jet impact region, the transfer of manganese from metal to slag was found to be increasing in the initial part of the blow for 200 t converter data reported by Cicutti *et al*.[24] However, a decreasing trend has been observed for the 55 t converter operation during the initial stage. The difference in the Mn refining profile by jet impact zone during the starting period may be due to the difference in lance practice adopted in the different converters. In Cicutti's heat data the lance position has started with high (2.5 m) and then lowered to the low position (2.2 m) after 4 minutes of blowing. However, in Holappa's data, the lance position was started with low position (0.9 m) and then raises to a high position (1.1 m) after 5 minutes. Decreasing in lance height increases the cavity area and thus enhances the kinetics of Mn reaction at jet impact region, which was reflected in Cicutti's heat data. A similar trend of refining profile of Mn in jet impact area for the intermediate and final stage of converter operation has been observed for both the heats. The increase in Mn refining during the middle stage of the blow and finally decreasing towards the end blow period may be caused by the reduction in the jet impact temperature which exerts a substantial effect on the overall mass transfer coefficient ($k_m$) of Mn reaction kinetics.

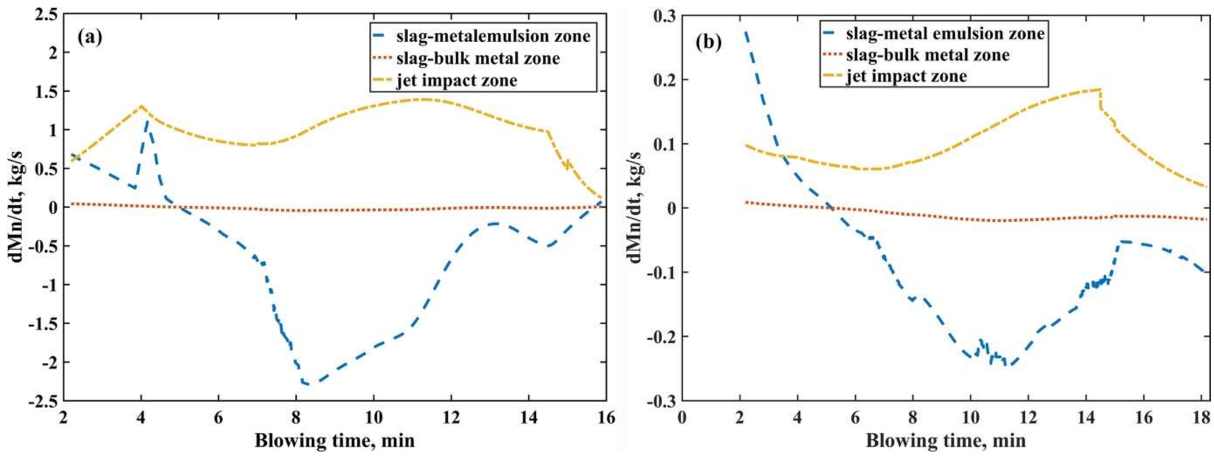


Figure 8: Mn removal rate calculated from different zones of the converter as a function of blowing time (a) 200 t converter (b) 55 t converter

The manganese removal rate by the circulating metal droplets in the emulsion has been computed for both cases and shown in Fig. 8. As seen from the figure, during the initial part, up to 5 min after the start of blowing, the rate of manganese transfer was found to be positive, which indicates the oxidation of manganese has been favored during this period. The transfer of manganese from metal droplet to slag is possible due to the low value of $[\text{wt pct Mn}]^{i}$ as a result of low temperature, high FeO, and low basicity during this period. However, as the blow progresses, the droplet surface temperature raises, FeO in slag decreases due to rapid decarburisation and as a result basicity increases, which initiates the conditions for the reversion of MnO from slag to the metal droplets. A significant fraction of manganese has been observed to be transferred from slag to metal by the emulsion phase during the middle stage of the blow. The peak reversion has been found to take place during 50 to 60% of blowing time. At the end stage of the blow, due to a small value of residence time of metal droplets in the emulsion, the rate of manganese transfer by the droplets approaches to zero. Further, it has been observed that the rate of manganese transfer in the slag-bulk metal zone is almost negligible as compared to jet impact and emulsion zone refining during the entire blow period. The reason may be due to the availability of a small area for the reaction that limits the kinetics of Mn refining in this zone. In the heat data provided by Holappa et al. for the 55 t LD-converter, the total iron oxide in the slag was observed to decrease (end blow $Fe_tO$ ~12 wt pct) during the last stage of the blow. Since the oxygen flow rate was held constat, the decreasing of slag iron oxide may be resulted from the lowering in lance position (1.25 m to 1.1 m) during 14 to 18 min of blowing. However, in Cicutti's heat no variation in oxygen flow rate and lance height was made during the last stage of the blowing and an increasing iron oxide trend was reported (end blow $Fe_tO$ ~22 wt pct). The variation in the iron oxide evolution in two different converters may be the reason for the difference in Mn refining prediction during the last 2 min of the blowing shown in Fig. 8. Due to low iron oxide in slag, the Mn refining prediction in Holappa's heat shows a reversion during the final stage of the blowing.

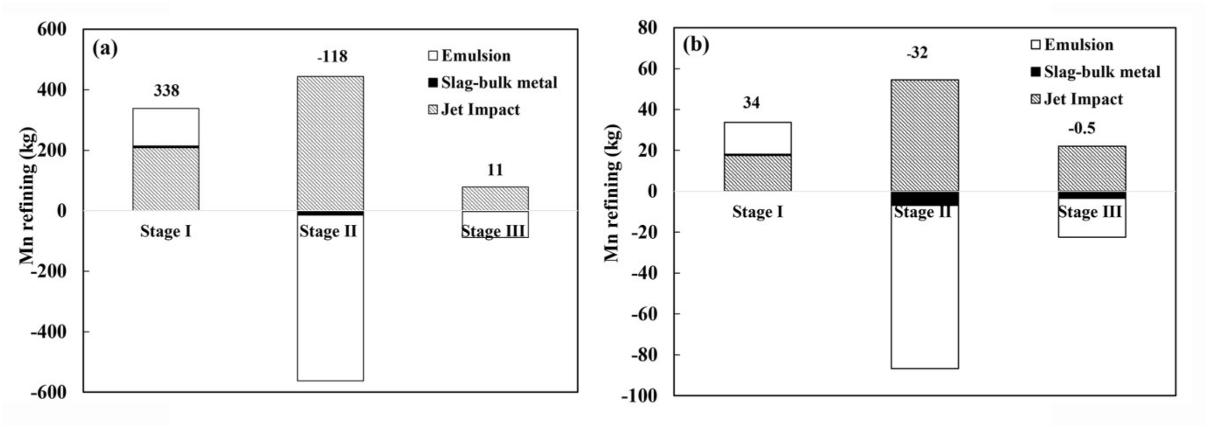


Figure 9: Total Mn exchange between metal and slag at different stages of the blowing (a) 200 t converter (b) 55 t converter

The total amount of manganese removed by each reaction zone during different stages of the blow has been computed by using the mathematical model. Based on the observed Mn profile, the entire blowing period has been divided into three stages: Stage I (0 to 30% of blow), Stage II (30 to 80% of blow), and stage III (80 to 100% of blow). Total Mn refining by each reaction zone has been obtained from the **Fig. 9** by computing the area under the curve in the three different regimes of blowing. The result shows that there is always a positive thermodynamic force for manganese oxidation during the initial stage of the blow. The enhanced manganese refining observed at the beginning of the blow is caused by oxidation of droplets in the emulsion in addition to the oxidation in jet impact region. The competition between the oxidation and reduction particularly in the jet impact zone and emulsion determines the direction of manganese transfer in second and end stage of the blow. In the middle stage of the blow, it has been observed that the reduction of MnO by the metal droplets dominates, which was found to be the main reason for a manganese reversion from slag to metal.

### 7.3. Analysis of Mn reaction kinetics in emulsion

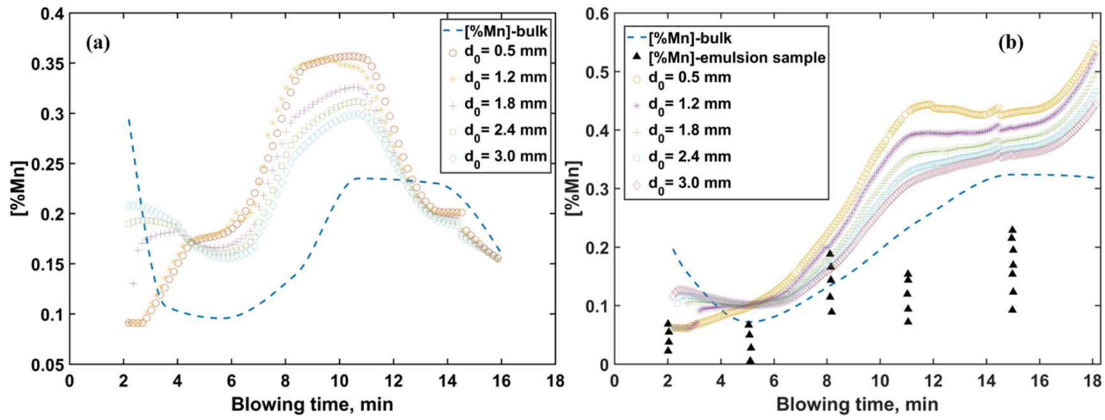


Figure 10: Mn refining of a metal droplet inside the emulsion phase; the dotted line represents the bulk concentration (measured) and the other symbols represent the concentration of Mn in the droplet at the time of returning to the bath (simulated) (a) 200 t converter data (b) 55 t converter data; the solid symbol represents the measured Mn in emulsion

The kinetics of manganese transfer between metal droplets and the slag is dependent on the interfacial concentration, the size of initial droplets and their bloating behavior as a result of decarburization reaction**. Figure 10** shows the concentration of Mn in the refined droplets of different sizes as a function of blowing time. As can be seen from the figure, the manganese concentration of the droplets at the time of return to the bulk melt nearly follows the refining path of Mn in the bulk metal for both the converters under investigation. Further, it was observed that the rate of oxidation or reduction of smaller sized droplets is higher as compared to the larger ones. The reason for this may be due to longer residence time and high surface area/volume ratio associated with smaller sized droplets. [21] As a result of which the reactions in small-sized droplets approaches the equilibrium concentration quickly. However, the big droplets having small residence time and surface area to volume ratio do not complete equilibrium and consequently contribute less towards the conversion process.[21] The fast rate of decarburisation associated with the droplets of diameter of the range ~0.5 mm (predicted decarburisation efficiency is more than ~70% during the entire blowing period)[21] accelerates the bloating process and thus results in increasing the reaction time between the droplet and slag to achieve the final equilibrium Mn concentration.

The present result agrees well with the observation made by Millman *et al.*[47] in a 6 t pilot scale converter experiments. The authors reported that during the middle blow period (after 10 min) the Mn pick up from the slag to droplet takes place for specific size range (1 to 3 mm) in the emulsion layer. The present model calculation predicts that the Mn pick up by the droplets in the lower region of the size spectrum makes a greater contribution to the reversion process.

Holappa *et al.* [42] measured the manganese concentration in the emulsion during the blowing time which has been shown in **Fig. 10 (b).** It can be seen that during the initial stage of the blow the predicted value of droplet manganese concentration agrees reasonably well with the measured concentration in the emulsion, whereas a difference between the predicted and the measured value has been observed at an intermediate stage of blowing. The cause of this deviation could not be explained by this study since a significant reversion of bulk Mn concentration has been observed during middle and end stage of blowing, although the emulsion Mn concentration shows a lower value than the bulk. It is noteworthy that the reported manganese concentration in the emulsion represents the average concentration of the droplets in the emulsion at a particular instance of blowing time, whereas the predicted Mn by the model is the concentration of refining droplets (at the time of re-entry to the bath). This could be one of the reasons for the difference between the model prediction and actual measurement.

### 7.4 . Model validation with the measured hot metal composition

The rate of manganese refining from three different zones are combined and mass balance has been applied in the hot metal to compute the bath Mn concentration (in wt pct) at each time of blowing. The model prediction of change in concentration of Mn in the bulk metal as a function of blowing time is shown in **Fig. 11.** The model calculation of Mn has been compared with the actual Mn value measured in the hot metal for two different converters. As can be seen from the **Fig. 11. (a),** in Cicutti's heat data, the predicted Mn matches well with the actual Mn particularly during the early part of the blow. However, a small deviation has been observed towards the end of the blow. It may be due to the inaccurate calculation of manganese equilibrium at slag-metal droplet interface. Further experimental studies are needed to establish the manganese distribution between the slag and metal droplet in the emulsion. This model has also been applied to a different converter of 55 t capacity. As shown in **Fig. 11. (b),** good agreement between the measured and predicted values was observed. It should be noteworthy to mention that in contrast to the difference between the emulsion sample measurement and the refined droplets (in **Fig 10. (b)**), Jalkanen *et al.*'s heat data[48] of Mn refining of bulk metal profile shows a great consistency with the predicted values. Several authors indicated that the way the samples (in a blow, after blow stopping, height and time of sampling) are collected from the emulsion, can have a significant influence on droplet characteristics. [49, 50] However, the sampling procedure was not mentioned in Jalkanen's study and thus the substantial reversion observed in the bulk metal due to the cause of slag/metal droplet reversion as predicted by the model, was not conclusively verified. This needs a further experimental study to investigate the reversion mechanism of Mn to establish the current hypothesis.

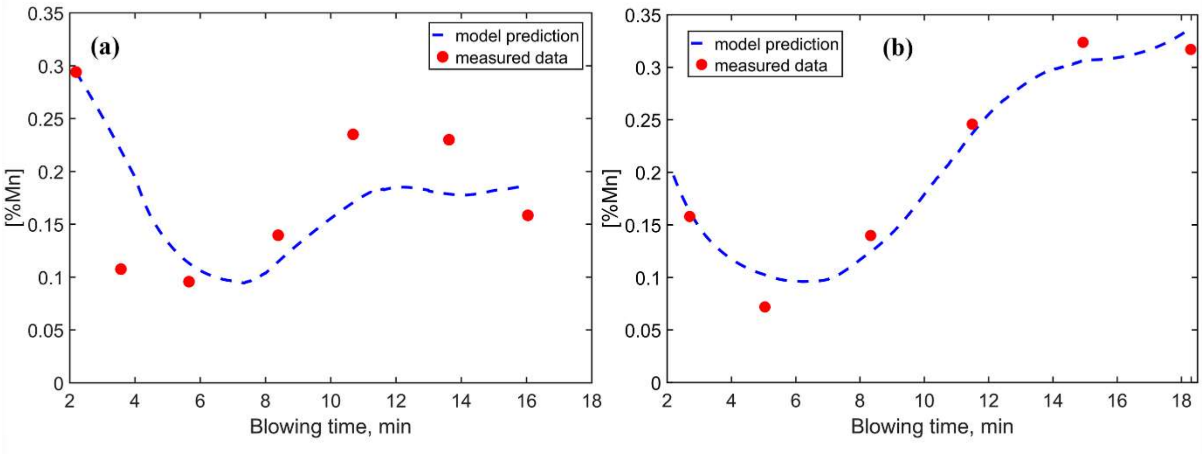


Figure 11: Model validation of Mn prediction in hot metal (a) Cicutti *et al.* data[24] (b) Jalkanen *et al.* data[46]

## 8. Conclusions

A kinetic model for Mn reaction in BOF has been developed. The computational model can predict the change in manganese concentration in the bulk metal during the blow period by estimating the rate of refining from different zones of the converter. The following conclusions are made from this study:

1. The temperature at the slag–metal droplet interface plays a major role in deciding the oxidation and reduction behaviour of Mn reaction. Higher interface temperatures lead to decrease in thermodynamic driving force for the mass transfer from metal droplets to slag.
2. The kinetics of Mn refining in the first stage of the blow is controlled by the oxidation of Mn by FeO in the emulsion and direct oxidation of Mn by $O_2$ in the jet impact zone.
3. Competition between the Mn oxidation in the jet impact zone and reduction of MnO by Fe in the metal droplets in emulsion zone determines the direction of Mn transfer during middle and end period of the blow.
4. In the middle stage of the blow, after 30 to 40 % of blowing, a significant fraction of Mn reversion was observed to take place in the emulsion zone. Due to a large increase in temperature of the droplet-slag interface, the reaction (Eq. 1) proceeds in the reverse direction which was found to be the primary reason for manganese reversion.
5. During the last stage of the blow, the refining of Mn is a result of simultaneous reaction at jet impact and emulsion zones. The reaction (Eq. 1) direction at slag-metal droplet interface controls the conversion process in this period.
6. The rate of Mn oxidation in the emulsion is predicted to be a strong function of droplet diameter and the residence time. Small sized droplets have high conversion capacity than the large diameter ones.

**Acknowledgement**

The authors acknowledge their gratitude to Tata Steel for providing financial support for this work.

**Nomenclature**

A-Area of the reaction interface ($m^2$)
$C_{p,m}$ – Heat capacity of bulk metal (J/kg)
$C_{p,s}$ – Heat capacity of slag (J/kg)
$d_p$ – Diameter of the droplet (m)
$\left(\frac{dMn}{dt}\right)_{overall}$ – Overall manganese refining rate (kg/s)
$\left(\frac{dMn}{dt}\right)_{iz}$ - Manganese refining rate in jet impact zone (kg/s)
$\left(\frac{dMn}{dt}\right)_{sm}$ - Manganese refining rate in slag-bulk metal zone (kg/s)
$\left(\frac{dMn}{dt}\right)_{em}$ - Manganese refining rate in emulsion zone (kg/s)
$J_{Mn}$ – Manganese reaction rate (kg/s)
H- Bath height (cm)
L- Bath diameter (cm)
$k_{overall}$- Overall mass transfer coefficient (m/s)
$k_m$ – Mass transfer coefficient in metal phase (m/s)
$k_m^{drop}$- Mass transfer coefficient of metal droplet (m/s)
$k_{overall}^{em}$- Overall mass transfer coefficient in emulsion (m/s)
$k_s$ – Mass transfer coefficient in slag phase ($ms^{-1}$)
$k'_{Mn}$ – Apparent equilibrium constant of Mn (-)
K – Equilibrium constant (-)
$L_{Mn}$ – Equilibrium manganese partition ratio (-)
$[\%Mn]^{eq}$ – Equilibrium manganese concentration (wt pct)
$[\%Mn]^{i}$ – Manganese concentration at slag metal interface (wt pct)
$P_{O2}$ – partial pressure of oxygen inside the furnace (atm)
$N_p^{eject,t}$ – Number of droplets of $p^{th}$ class size ejects to the bath at blowing time t (-)
$N_p^{return,t}$ – Number of droplets of $p^{th}$ class size returns to the bath at blowing time t (-)
P- Number of divisions in the droplet size spectrum (-)
Re- Reynolds number (-)
$R_{B,T}$- Droplet generation rate (kg/s)
Sc- Schmidt number (-)
Sh- Sherwood number (-)
$t_{res}$- Residence time of droplet in emulsion (seconds)
$T_m$- Temperature of the hot metal (K)
$T_{iz}$- Temperature at the impact zone (K)
$T_{drop}$ -Interface temperature at slag–metal droplet (K)
$T_\infty$- Temperature in the emulsion medium (K)
$T_0$ - Initial temperature of the metal drop at the time of ejection (K)
u- Velocity of the droplet (m/s)
$W_b$ – Weight of bulk metal (kg)
$W_{Mn}^{eject,t}$- Mass of metal ejected into emulsion at time t (kg)
$W_{Mn}^{return,t}$- Mass of metal droplet returns to the bulk metal at time t (kg)

**Greek symbols**

$\rho_m$ – Density of the bulk metal ($kg/m^3$)

$\rho_s$ – Density of slag ($kg/m^3$)

$\lambda_m$- Thermal conductivity of liquid metal (W/m K)

$\lambda_s$ - Thermal conductivity of slag (W/m K)

ε – Stirring energy (W/t)

μ - Viscosity (Pa.s)

**Subscripts and Superscripts**

**cav- Cavity**

eq- Equilibrium

em- Emulsion

gm- Gas/metal

i- Interface

iz- Impact zone

m- Hot metal

sc- Scrap

sm-Slag/metal

## References


1. A.T. Morales and R. J. Fruehan: *Metall. Mater. Trans. B,* 1997, vol. 28, pp. 1111-18.
2. D. S.Kumar, R. Sah, V. R. Sekhar and S. C. Vishwanath: *Transactions of the Indian Institute of Metals,* 2016, vol. 69, pp. 775-82.
3. H. Suito and R. Inoue: *ISIJ Int.* 1995, vol. 35, pp. 266-71.
4. H. Suito and R. Inoue: *Transactions of the Iron and Steel Institute of Japan,* 1984, vol. 24, pp. 257-65.
5. H. Suito and R. Inoue: *Transactions of the Iron and Steel Institute of Japan,* 1984, vol. 24, pp. 301-07.
6. M. Meraikib: *ISIJ Int.*, 1993, vol. 33(3), pp.352-360.
7. A. Sobandi, H. G. Katayama and T. Momono: *ISIJ Int.*, 1998, vol. 38 (9), pp. 953–958.
8. S. H. Kim and B. Song. *Metall. Mater. Trans. B*, 1999, 30(3), pp.435-442
9. C. Zhu, G. Li, Z. Chen, G. Ma and J. Liu: *ISIJ Int.,* 2008, vol. 48, pp. 123-29.
10. S. Jung: *ISIJ Int.* 2003, vol. 43, pp. 216-23.
11. S. C. Duan, C. Li, X. L. Guo, H. J. Guo, J. Guo and W. S. Yang: *Ironmak. Steelmak.*, 2017, pp.1-10.
12. W. L. Daines and R. D. Pehlke: *Metall. Trans.,* 1971, vol. 2, pp. 1203-11.
13. R. J. Pomfret and P. Grieveson: *Ironmak. Steelmak.,* 1978, vol. 5, pp. 191-97.
14. K. Xu, G. Jiang, W. Ding, L. Gu, S. Guo, and B. Zhao: *ISIJ Int.*, 1993, vol. 33, no. 1, pp. 104–108.

15. E. Shibata, H. Sun and K. Mori: *Metall. Mater. Trans. B,* 1999, vol. 30, pp. 279-86.

16. M. Vargas-Ramirez, A. Romero-Serrano, F. Chavez-Alcala, B. Zeifert and M. Hallen-Lopez: Steel Res. Int., 2002, vol. 73(9), pp : 378-384.

17. T. Takaoka, I. Sumi, Y. Kikuchi and Y. Kawai: *ISIJ Int.,* 1993, vol. 33, pp. 98-103.

18. B. K Rout, G. Brooks, M. A. Rhamdhani, Z. Li, F.N. H. Schrama and J. Sun: *Metall. Mater. Trans. B*, 2018, pp. 1-21.

19. G. Brooks, Y. H. Pan, Subagyo and K. Coley: *Metall. Mater. Trans. B,* 2005, vol. 36, pp. 525-35.

20. B. K. Rout, G. A. Brooks, M. A. Rhamdhani and Z. Li: *Metall. Mater. Trans. B*, vol 47 (6), pp. 3350-61.

21. B. K Rout, G. Brooks, M. A. Rhamdhani, Z. Li, F. N. H. Schrama and A. Overbosch: Metall. Mater. Trans. B, 2017 (accepted).

22. A. I. van Hoorn, J. T. van Konyneburg and P. J. Kreijger, *Proc. McMaster Symposium on " The role of slag in Basic Oxygen Processes"*, Hamilton, 1976.

23. H. Jalkanen, *In Sohn International Symposium:Advanced Processing of Metals and Materials Volume 2: Thermo and Physicochemical Principles: Iron and Steel Making*, 2006, Vol. 2, pp. 541-554.

24. C. Cicutti, M. Valdez, T. Pérez, J. Petroni, A. Gómez, R. Donayo and L. Ferro: *Sixth International Conference on Molten Slags, Fluxes and Salts*, ed. ISS (Stockholm-Helsinki: Warrandale, PA, 2000).

25. Y. Kawai, N. Shinozakiand K. Mori: Canadian Metallurgical Quarterly, 1982, vol. 21(4), pp.385-391.

26. N. Shinozaki, K. Mori and Y. Kawai: *Tetsu-to-Hagane(Journal of the Iron and Steel Institute of Japan),* 1982, vol. 68, pp. 72-80.

27. S. V. Komarov and V. V. Yakovlev: *Steel USSR,* 1984, vol. 14, pp. 316-17.

28. F. E. Rote and R. A. Flinn: *Metall. Trans.,* 1972, vol. 3, pp. 1373-84.

29. F. Oeters: *Steel Res.* 1985, vol. 56, pp. 69-74.

30. B. K. Rout, G. A. Brooks, Z. Li and M. A. Rhamdhani: *AISTech - Iron and Steel Technology Conference Proceedings*, 2015, vol. 3, pp 3225-37.

31. S. Ban-Ya: *ISIJ Int.,* 1993, vol. 33, pp. 2-11.

32. K Chiba, A. Ono, M Saeki, M. Yamauchi, M. Kanamoto and T. Ohno: *Ironmak. Steelmak.,* 1993, vol. 20, pp. 215-20.

33. M. Ishikawa: *ISIJ Int.,* 2004, vol. 44, pp. 316-25.

34. S. Kitamura, T. Kitamura, K. Shibata, Y. Mizukami, S. Mukawa and J. Nakagawa: *ISIJ Int.* 1991, vol. 31, pp. 1322-28.

35. S. C.Koria: *Canadian metallurgical quarterly*, 1992, vol. 31, no. 2, pp. 105-112.

36. Y. Ogasawara, Y. Miki, Y. Uchida and N. Kikuchi: *ISIJ int.*, 2013, vol. 53, no. 10, pp. 1786-1793.

37. M. Ishiguro: *Tetsu-to-Hagane,* 1971, vol. 57, pp. 267-70.

38. S. C. Koria and K. W. Lange: *Steel Res.* 1987, vol. 58, pp. 421-26.

39. F. Oeters. *Metallurgy of steelmaking*. Verlag Stahleisen, 1994, pp. 316-77.

40. S. C. Koria and K. W. Lange: *Metall. Trans. B,* 1984, vol. 15, pp. 109-16.

41. B. T. Chao, *Journal of Heat Transfer* 1969, vol. 91, pp. 273-80.

42. L. Holappa and P. Kostamo: *Scand. J. Metallurgy,* 1974, vol. 3, pp. 56-60.

43. N. Dogan, G.A. Brooks, and M.A. Rhamdhani: *ISIJ Int.*, 2011, vol. 51, pp. 1086–92.

44. Slag Atlas, *Verlag Stahleisen GmbH, Düsseldorf* 1995, pp. 345-346.

45. A. Kondratiev and E. Jak: *Metall.Mater. Trans. B,* 2001, vol. 32, pp. 1015-25.

46. N. Dogan, G. A. Brooks, and M. A. Rhamdhani: *ISIJ Int.*, 2009, vol. 49, no. 10, pp. 1474–82.

47. M. S. Millman, A. Kapilashrami, M. Bramming and D. Malmberg: *Imphos: Improving Phosphorus Refining*, European Union, Luxembourg, 2011.

48. H. Jalkanen and L. Holappa, In *VII International Conference on Molten Slags Fluxes and Salts, The South African Institute of Mining and Metallurgy*, (2004).

49. S. Sabah and G. Brooks: *Metall. Mater. Trans. B,* 2015, vol. 46, pp. 863-72.

50. S. Spooner, J. M. Warnett, R. Bhagat, M. A. Williams and S. Sridhar: *ISIJ Int.,* 2016, vol. 56, pp. 2171-80.

## Appendix:

### A1. Calculation of total stirring energy:

The following equations have been applied to estimate the stirring power due to the combined effect of both top and bottom blowing [40]:

$$\epsilon = \epsilon_t + \epsilon_b \tag{A1}$$

$$\epsilon_t = 6.32 \times 10^{-7} \cos(\alpha) \frac{Q_{O2} M_{O2}}{W_b n_n^2 d_t^3 L_h} \tag{A2}$$

$$\epsilon_b = \frac{6.18 Q_b T_m}{W_b} \left(\ln\left(1 + \frac{\rho_m g H}{P_a}\right) + \left(1 - \frac{T_b}{T_m}\right)\right) \tag{A3}$$

Where $\varepsilon_t$ and $\varepsilon_b$ are the specific mixing power (W/t) due to top and bottom gas injection respectively. α is the angle of the lance with the vertical axis (rad), $Q_{O2}$ is the oxygen flow rate ($Nm^3$/min), nn is the number of nozzles in the lance tip, $d_t$ is the throat diameter (m), $L_h$ is the lance height from the bath level (m), $Q_b$ is the bottom blowing rate ($Nm^3$/min), $P_a$ is the atmospheric pressure (atm) and $T_b$ is the temperature of the injected bottom gas.

### A.2. Input data used for model validations

**Caption List**

**List of Figures**

**Figure 1**: Schematic of Mn transfer across slag-metal interface

**Figure 2**: Comparison of actual Mn in the metal and the interfacial Mn calculated from Suito's equilibrium distribution models: Slag and hot metal composition data were taken from a top blowing process

**Figure 3**: Schematic representation of oxidation/reduction reactions of Mn across various interfaces in a BOF**Figure 4**: Transport process of Mn at metal drop and slag containing iron oxide interface in the emulsion zone

**Figure 5**: Calculation steps for Mn refinement model for a BOF process

**Figure 6**: Typical manganese refining path in a top blowing converter. [22, 24] Region I: rapid manganese oxidation, Region II- manganese reversion from slag to metal, Region III: manganese oxidation

**Figure 7**: Effect of temperature on the equilibrium manganese at slag-metal interface (solid line- actual Mn in bath, dotted line- interfacial Mn concentration estimated at different slag-metal interface temperatures), $T_m$- Hot metal temperature (as measured during blowing time) and T is the interface temperature

**Figure 8**: Mn removal rate calculated from different zones of the converter as a function of blowing time (a) 200 t converter (b) 55 t converter

**Figure 9**: Total Mn exchange between metal and slag at different stages of the blowing (a) 200 t converter (b) 55 t converter

**Figure 10**: Mn refining of a metal droplet inside the emulsion phase; the dotted line represents the bulk concentration (measured) and the other symbols represent the concentration of Mn in the droplet at the time of returning to the bath (simulated) (a) 200 t converter data (b) 55 t converter data; the solid symbol represents the measured Mn in emulsion

**Figure 11**: Model validation of Mn prediction in hot metal (a) Cicutti's data[24] (b) Jalkanen and Holappa. data[48]

**List of Tables**

Table 1: Possible reactions and their direction for Mn refining in BOF operation

| **Reaction/stages** | **Reaction 1 (Emulsion)** | **Reaction 3 (Jet impact zone)** |
|---|---|---|
| Stage I (0 – 30%) | Forward (Mn flows from metal to slag | Forward (Mn flows from metal to slag) |
| Stage II (30- 80%) | Forward/Backward – Depends on slag composition and T | Forward (Mn flows from metal to slag) |

| | | |
|---|---|---|
| Stage III (80-100%) | Forward/Backward – Depends on slag composition and T | Forward (Mn flows from metal to slag) |

Table A1: Input data for model calculation: Cicutti *et al.* [24]

| **Input parameters** | **Value** |
|---|---|
| Initial hot metal composition (Blowing time = 2.2 min) | 170000 kg, wt pct C= 3.86, wt pct Si = 0.19, wt pct Mn = 0.29, wt pct P = 0.065 |
| Scrap composition | 30000 kg, wt pct C = 0.08, wt pct Si = 0.001, wt pct Mn = 0.52 |
| Hot metal temperature | 1623- 1923 K (1350- 1650 °C) |
| Initial slag composition and weight | Initial slag weight at 2.2 min = 5200 kg, total lime added = 7600 kg, Iron ore = 1900 kg, Quartzite = 800 kg<br>Slag composition : wt pct CaO = 27, wt pct FeO = 33, wt pct $SiO_2$ = 17, wt pct MnO = 13.5, wt pct MgO = 5, wt pct $P_2O_5$= 4.5 |
| Oxygen blow | 620 $Nm^3$/min, six hole lance |
| Bottom blow (Ar/$N_2$) | 2.5 – 8.33 $m^3$/min |
| Lance height | 2.5, 2.2, 1.8 m |
| Steel density | 7000 kg/$m^3$ |
| Slag density | Partial molar volume method [44] |
| Surface tension of steel | 1.7 N/m |
| Viscosity of slag | Modified Urbain model [45] |
| Diffusion coefficient in metal phase at 1873K (1600 °C) | C- 2.0 × $10^{-9}$ $m^2$/s, Si – 3.8× $10^{-9}$ $m^2$/s, Mn - 7× $10^{-9}$ $m^2$/s, P-4.7× $10^{-9}$ $m^2$/s |
| Gas fraction in emulsion | 0.8 |
| Droplet diameter | 2.3×$10^{-4}$ m to 3.35× $10^{-3}$ m |
| Angle of droplet ejection | 60 degree |

Table A2: Input data for model calculation: Holappa *et al.* [40]

| Input parameters | Value |
|---|---|
| Initial hot metal composition (Blowing time = 2.2 min) | 48000 kg, wt pct C= 3.88, wt pct Si = 0.073, wt pct Mn = 0.2, wt pct P = 0.026 |
| Scrap composition | 5000 kg, wt pct C = 0.08, wt pct Si = 0.001, wtpct Mn = 0.52 |
| Hot metal temperature | 1603- 1973 K (1330- 1700 °C) |
| Slag composition and weight | Initial slag weight at 2.2 min = 1376 kg, Iron ore = 900 kg (dust) Dynamic slag data |
| Oxygen blow | 130 $Nm^3$/min, three-hole lance, lance angle 15 degree |
| Bottom blow ($Ar/N_2$) | 0 |
| Lance height | 1.0m, 1.1m, 1.2m, 1.5m |
| Steel density | 7000 $kg/m^3$ |
| Slag density | Partial molar volume method [44] |
| Surface tension of steel | 1.7 N/m |
| Viscosity of slag | Modified Urbain model [45] |
| Diffusion coefficients | C- $2.0 \times 10^{-9}$ $m^2/s$, Si – $3.8\times 10^{-9}$ $m^2/s$, Mn - $7\times 10^{-9}$ $m^2/s$, P- $4.7\times 10^{-9}$ $m^2/s$ |
| Gas fraction in emulsion | 0.8 |
| Droplet diameter | $2.3\times10^{-4}$ m to $3.35\times 10^{-3}$ m |
| Angle of droplet ejection | 60 degree |